THE JOURNAL OF BIOLOGICAL CHEMISTRY
Vol. 277, No. 18, Issue of May 3, pp. 15579–15585, 2002
Printed in U.S.A.

Effect of Phosphorylation on the Structure and Fold of Transactivation Domain of p53*

Received for publication, July 23, 2001, and in revised form, February 7, 2002
Published, JBC Papers in Press, February 19, 2002, DOI 10.1074/jbc.M106915200

Sanchari Kar‡§, Kazuyasu Sakaguchi¶, Yasuyuki Shimohigashi¶, Soma Samaddar‡§, Raja Banerjee‡‖, Gautam Basu‡, V. Swaminathan§‡‡, Tapas K. Kundu‡‡§§, and Siddhartha Roy‡**¶¶**

From the ‡Department of Biophysics, Bose Institute, P-1/12 C. I. T., Scheme VII M, Calcutta 700 054, India, the ¶Laboratory of Structure-Function Biochemistry, Department of Chemistry, Faculty of Sciences, Kyushu University, Fukuoka 812-8581, Japan, and the ‡‡Transcription and Disease Laboratory, Molecular Biology and Genetics Unit, Jawaharlal Nehru Center for Advanced Scientific Research, Jakkur, Bangalore 560064, India

Several phosphorylations are known to occur in the N-terminal transactivation domain of human p53. To explore the structural effects of these phosphorylations, we have chemically synthesized the unphosphorylated p53-(1–39) and its three phosphorylated analogs, phosphorylated at Ser-15, Thr-18, and Ser-20. p53-(1–39) and its Ser-15 and Thr-18 phosphorylated analogs were tested for interaction with p300. The order of binding affinities was similar to that derived from biochemical experiments with the whole protein, indicating functional integrity of the domain. Differences in chemical shifts and coupling constants indicate significant structural changes upon phosphorylations. The single tryptophan in the unphosphorylated domain has an emission maximum and a Stern-Volmer constant that are characteristics of tryptophans situated in protein interiors. The diffusion constant is monomer-like, with an axial ratio of 1:7.5, indicating a significant degree of compaction. Upon phosphorylations, the emission maximum and diffusion constant change significantly toward values that indicate more open conformations. Binding of the hydrophobic probe bis-1-anilino-8-naphthalenesulfonate to the unphosphorylated and one of the phosphorylated domains is also significantly different, suggesting different conformations. We propose that phosphorylations switch the largely folded transactivation domain to more open conformations that interact with transcription factors such as p300/cAMP-responsive element-binding protein-binding protein, leading to enhancement of gene expression.

p53 lies at the center of the cellular response to genotoxic stress. Various stress signals integrate by means of post-translational modifications of the p53 protein, resulting in different downstream responses (1). A major response is to halt cell cycle progression with corresponding activation of genes needed for DNA repair. A second kind of response is apoptosis (2). Genotoxic stresses activate many cellular kinases that phosphorylate various serine and threonine residues in p53, as well as enzymes that cause lysine acetylations (3). Presently, at least 12 serine/threonines and 2 lysines are known to be modified in p53 and there may be more modification sites. This signaling system and the code of post-translational modification are still incompletely understood (1). An understanding of the structural basis of such signal integration and transduction remains a distant dream.

p53 is a multidomain protein. The N-terminal domain 1–73 is responsible for transactivation function and binding of such proteins as Mdm2/Hdm2, which down-regulate the levels of p53 (4). The N-terminal domain of p53 is emerging as one of the most important regions in p53 function. One of the major pathways of transactivation is through interaction with p300/CBP[1] and recruitment of this protein to the required promoter region. p300/CBP has well known histone acetyltransferase activity, which results in histone acetylation and remodeling of the chromosome in that region leading to enhanced transcription (5). Clearly, interactions of the N-terminal domain of p53 with Mdm2 and p300/CBP and possibly with other regulatory proteins are of crucial importance in understanding the various roles played by p53 as the guardian of the genome.

Although crystal or NMR structures of other domains have been reported (6, 7), very little is known about the structure of this important domain. Only very recently, an NMR study of this domain has shown this to be disordered, although the authors concluded that secondary structural elements are present (8). It now appears that there are at least eight phosphorylation sites within the N-terminal subdomain: serines 6, 9, 15, 20, 33, 37, and 46 and threonine 18 (1). Functions of several of these phosphorylations are not clear. However, it appears that the Ser-15 phosphorylation plays a crucial role in the transactivation process (9–11). Phosphorylation of Ser-15 occurs very soon after initial stressing of the cells (12). Among

* This work was supported in part by the Nissan Science Foundation and a grant-in-aid for scientific research (to K. S.). The costs of publication of this article were defrayed in part by the payment of page charges. This article must therefore be hereby marked "*advertisement*" in accordance with 18 U.S.C. Section 1734 solely to indicate this fact.

§ Recipient of a Council of Scientific and Industrial Research, India (CSIR) junior research fellowship.

‖ Permanent address: Dept. of Chemistry, St. Xaviers College, Calcutta 700016, India.

** Recipient of a grant from the Department of Atomic Energy, Government of India.

§§ Recipient of a grant from CSIR.

¶¶ To whom correspondence should be addressed. Tel.: 91-33-412-1261; Fax: 91-33-334-3886; E-mail: sidroy@vsnl.com or sidroy@boseinst.ernet.in.

[1] The abbreviations used are: CBP, cAMP-responsive element-binding protein-binding protein; Pep53, peptide corresponding to residues 17–28 of human p53; Bpep53, same peptide as Pep53 except five α-aminoisobutyric acid residues incorporated in designated positions; Aib, α-aminoisobutyric acid; Ser15P, p53-(1–39) domain phosphorylated at serine 15; Thr18P, p53-(1–39) domain phosphorylated at threonine 18; Ser20P, p53-(1–39) domain phosphorylated at serine 20; Fmoc, fluorenyl methoxycarbamoyl; $D_{20,w}$, diffusion constant at 20 °C in water; ANS, 1-anilino-8-naphthalenesulfonate; HPLC, high performance liquid chromatography; TOCSY, total correlation spectroscopy; NOESY, nuclear Overhauser effect spectroscopy.

other things, this phosphorylation leads to phosphorylation of the Thr-18 by casein kinase-1 (13) and consequent inhibition of interaction of p53 with Mdm2 (14). Ser-15 phosphorylation also leads to greatly increased binding of p53 to CBP/p300. It is also possible that the phosphorylation of Ser-15 leads to an enhancement of acetylation of C-terminal lysines and has some effect on p53 mediated apoptosis (15). Such multiple effects of a single phosphorylation suggest that this phosphorylation may be causing a conformational change in the transactivation domain of the protein. Similarly, phosphorylation at Ser-20 has been implicated in various downstream responses (10, 16, 17).

In this study we have focused our attention on the structural consequences of the phosphorylation of Ser-15, Thr-18, and Ser-20 in the N-terminal domain. Because it is difficult to produce specifically phosphorylated derivatives of the whole protein, we have chosen to study the N-terminal subdomain 1–39, which can be chemically synthesized in phosphorylated forms in large quantities.

EXPERIMENTAL PROCEDURES

Materials

Fmoc amino acids were purchased from Novabiochem (San Diego, CA). Vydac C-8 column was purchased from Grace-Vydac (Hesperia, CA). All other materials were of high quality analytical grade.

Methods

Expression and Purification of p300—His^6-tagged recombinant full-length p300 was expressed in Sf21 insect cells by using the baculovirus expression system and purified by nickel-nitrilotriacetic acid affinity purification as described previously (18). Briefly, Sf21 cells were infected with the recombinant baculovirus for 72 h, following which they were harvested and homogenized in a homogenization buffer (10 mM Tris-HCl, pH 7.5, containing 10% glycerol, 0.1% Nonidet P-40, 2 mM β-mercaptoethanol, 2 mM phenylmethylsulfonyl fluoride, 50 μg/ml leupeptin, 50 μg/ml aprotinin, 500 mM NaCl, and 15 mM imidazole). The cleared lysate was bound to the nickel-nitrilotriacetic acid-agarose beads (Qiagen GmbH) and washed in the same buffer with 300 mM NaCl and 15 mM imidazole. The protein was eluted in the homogenization buffer containing 200 mM NaCl and 250 mM imidazole. The purified protein showed a single band upon Coomassie stain and Western blot. It was also fully functional by histone acetyltransferase assay.

Peptide Synthesis and Characterization—The p53-(1–39) peptide and its phosphorylated derivatives were synthesized by the solid phase method with Fmoc chemistry using a model 430A peptide synthesizer (Applied Biosystems, Foster City, CA). Phosphoserine was incorporated as Fmoc-Ser(PO(OBzl)OH)-OH, and phosphothreonine was incorporated as Fmoc-Thr(PO(OBzl)OH)-OH. Peptides were cleaved from the resin, and side-chain protecting groups were removed by incubating in reagent K (trifluoroacetic acid:phenol:thioanisole:H_2O:ethanedithiol, 82.5:5:5:5:2.5) for 3 h at room temperature. The p53-(1–39) peptide and its phosphorylated derivatives were purified by HPLC on a pH-stable Vydac C-8 column with 0.2% hexafluoroacetone-NH_4OH, pH 7.0, acetonitrile. The masses of peptides were confirmed by matrix-assisted laser desorption ionization time-of-flight mass spectrometry on a Voyager PR-HR (PerSeptive Biosystems, Framingham, MA).

Another truncated version of p53, Pep53-(17–28) and a variant (Bpep53; see below for the sequence) were synthesized in a Biolynx 4175-peptide synthesizer using Fmoc protocol. Amino acids, except those stated below, were used as N-terminal Fmoc-protected and C-terminally pentafluorophenyl ester-activated with *N*-hydroxybenzotriazole. α-Aminoisobutyric acid (Aib), Asp, and Thr were used in the COOH form using benzotriazole-1-yloxytrispyrrolidinophosphonium hexafluorophosphate as activating agent with *N*-hydroxybenzotriazole and *N,N*-diisopropyl ethylamine (1:1:2). The peptides were acetylated at the N terminus using acetic anhydride and triethylamine (1:1) and cleaved from the resin (Novasyn KA) with trifluoroacetic acid:ethanedithiol:anisole:phenol (94:2:2:2, v/v/v/w). Both the peptides were purified by reverse phase HPLC on C-18 (Waters Associates) column using 0–60% acetonitrile in 0.1% trifluoroacetic acid and characterized by NMR. The sequences of the two peptides are ETFSDLWKLLPE (Pep53) and BTFBDBWKBLBE (Bpep53), where B stands for Aib.

NMR Spectroscopy—All NMR spectra were taken in a Bruker DRX-500 NMR spectrometer equipped with a *Z*-field gradient probe. All measurements were done in high precision 5-mm NMR tubes in 10 mM phosphate buffer, pH 7.0, containing 100 mM NaCl in 90% H_2O and 10% D_2O. All NMR experiments were done at 27 °C, unless stated otherwise. TOCSY and NOESY spectra were measured using standard pulse sequences in the Bruker pulse library using WATERGATE water suppression method. The diffusion measurements were carried out by stimulated echo-based pulse sequence (90° gradient pulse, 90° delay for diffusion, 90° gradient pulse acquisition). Typical delay for diffusion was set at 200 ms (202.244 (= Δ in the equation below) ms counting finite length of the pulses) (19). The strength of the gradient (G) pulse was varied, and G^2 *versus* ln[intensity] was plotted. The strength of the gradient and the intensity are related by the following equation.

$$\ln I = -[\{\gamma \cdot G \cdot \delta\}^2 \cdot D \cdot \{\Delta - \delta/3\}] \quad \text{(Eq. 1)}$$

I is the intensity, γ is the gyromagnetic ratio, D is the diffusion constant, δ is the delay between the first two 90° pulses, Δ is the delay between two gradient pulses (includes delay for diffusion), and G is the strength of the gradient pulse. From the slope of the line, D can be calculated, because all other parameters are known. $D_{20,w}$ values were calculated according to Cantor and Schimmel (20). Perrin factors and hydrodynamic radii were calculated from diffusion constants according to Cantor and Schimmel (20). The temperature was 27 °C. $J_{NH\text{-}\alpha H}$ values were derived from double quantum-filtered COSY spectra according to Kim and Prestegard (21).

Circular Dichroism—CD spectra were measured in a Jasco J-700 spectropolarimeter in 10 mM phosphate buffer, pH 7, containing 100 mM NaCl. The cuvette path length was 2 mm. Temperature was 7.5 °C. The bandwidth was 2 nm, and scan speed was 20 nm/min.

Fluorescence Measurements—All fluorescence spectra were measured in a Hitachi F-3010 fluorescence spectrophotometer at ambient temperature (25 ± 1 °C), unless stated otherwise. Acrylamide quenching was done in 10 mM phosphate buffer, pH 7, containing 100 mM NaCl. The observed fluorescence values were corrected for volume change and inner filter effect. Inner filter effect was corrected using the formula $F_{corr} = F_{obs} \times \text{antilog}[(A_{ex} + A_{em})/2]$. The excitation wavelength was 295 nm, and the emission wavelength was 340 nm. Excitation and emission band passes were 5 nm each. The quenching data was fitted to the Stern-Volmer equation: $F_0/F = 1 + K_{sv}[Q]$, where F_0 is the fluorescence intensity at zero quencher concentration, F is the intensity at a given quencher concentration Q, and K_{sv} is the Stern-Volmer constant.

Bis-ANS binding was carried out in 10 mM phosphate buffer, pH 7.0, containing 100 mM NaCl. Excitation and emission band passes were set to 5 nm. 10 μM p53-(1–39) or Ser20P was titrated with increasing concentrations of bis-ANS, and fluorescence intensity at 490 nm was recorded. The excitation wavelength was 387 nm. Fluorescence intensities were corrected for volume changes and inner filter effect.

Interaction of p53-(1–39) Domain and Its Derivatives with p300—Ser15P was labeled with fluorescein isothiocyanate at low pH so that the modification may be primarily directed toward the N terminus (resulting from lower pK of the α-amino group (Ref. 22)). 7.7 μM Ser15P was mixed with 20-fold molar excess of fluorescein isothiocyanate in 5% v/v ethanol (final concentration) in 0.2 M potassium phosphate, pH 6.0, at 25 °C, with continuous stirring for 4 h. It was then centrifuged, and the supernatant was loaded on to a Sephadex G-25 column, equilibrated, and eluted with 20 mM Tris-HCl, pH 7.9, containing 100 mM KCl. For direct titration, 720 nM fluorescein-labeled Ser15P in 20 mM Tris-HCl buffer, pH 7.9, containing 100 mM KCl was titrated with p300, and the anisotropy was determined at each point. The excitation wavelength was 480 nm, and the emission wavelength was 520 nm. For the competition experiments, 360 nM labeled Ser15P was mixed with 360 nM p300 in 20 mM Tris-HCl, pH 7.9, containing 100 mM KCl buffer and incubated for 5 min. This buffer was different from the buffer used for other spectroscopic experiments, as p300 is known to be stable in this buffer. The anisotropy was then determined, followed by addition of increasing amounts of unlabeled competing peptide. The excitation and emission wavelengths were 480 and 520 nm, respectively. The excitation and emission band passes were 10 and 5 nm, respectively. Anisotropy (A) was calculated according to the following formula: $A = (I_{\parallel} - I_{\perp})/(I_{\parallel} + 2I_{\perp})$, where $I_{\parallel}$ is the fluorescence intensity with parallel polarizers (0/0) and $I_{\perp}$ is the fluorescence intensity with crossed polarizers (0/90).

RESULTS AND DISCUSSION

Because we have attempted to work with the isolated p53-(1–39) fragment, it is important to assess the structural and functional integrity of this isolated domain. The functional integrity of the 1–39 domain can be judged from its interaction

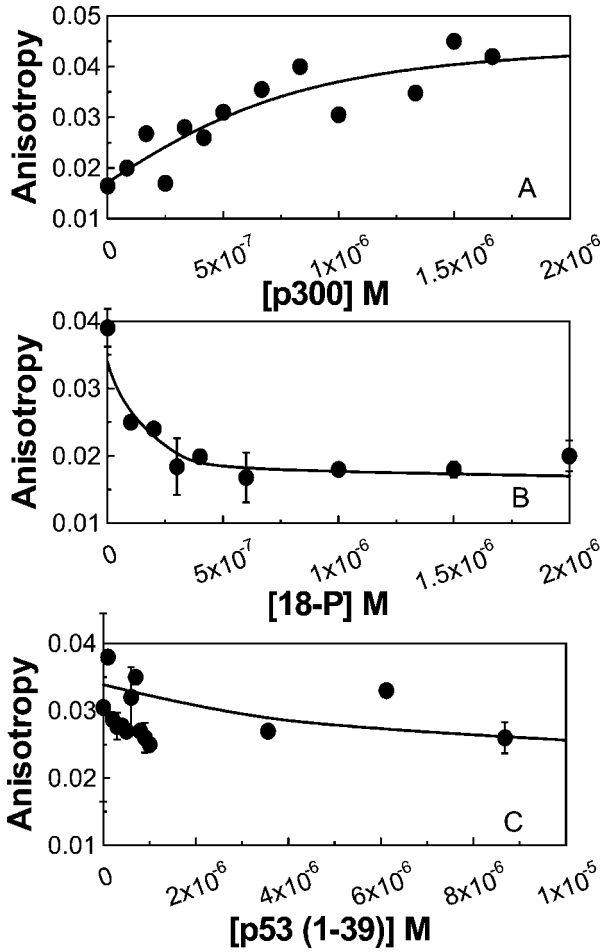

FIG. 1. **Binding of p300 with different phosphorylated derivatives of p53-(1–39).** *A*, titration of fluoresceinated Ser15P at a concentration of 720 nM with increasing concentrations of p300. The *line* shown is the best fit to a single-site binding equation. *B*, titration of 360 nM fluorescein-labeled Ser15P and 360 nM p300 complex with increasing concentrations of Thr18P and p53-(1–39) (*C*). *Lines* in *B* and *C* are merely polynomials and do not represent any binding equation. The solution conditions were 20 mM Tris-HCl, pH 7.9, containing 100 mM KCl. The temperature was 25 ± 1 °C. Excitation and emission wavelengths were 480 and 520 nm, respectively. The *error bars* are derived from three independent measurements. For clarity only every *third error bar* is shown.

with the natural receptors, *e.g.* TAF, Mdm2, or p300 (23). Previous reports have suggested that this domain binds to TAF and Mdm2 with high affinity (14, 24, 25). In addition, we have measured the binding of the 1–39 domain of p53 and two of its phosphorylated derivatives with p300. We have used fluoresceinated Ser15P peptide to measure binding by fluorescence anisotropy. Fig. 1*A* shows the titration of fluoresceinated Ser15P with increasing concentrations of p300. Anisotropy increased and then quickly saturated. When the data were fitted to a single-site binding equation, a dissociation constant of 81 nM was obtained. A qualitative estimate of binding constants of Thr18P and p53-(1–39) was obtained using competition with these unlabeled fragments. Fig. 1 (*B* and *C*) shows the decrease in anisotropy when a complex of p300 and fluoresceinated Ser15P, 360 nM each, was titrated with increasing concentrations of either unlabeled Thr18P or p53-(1–39). In the case of Thr18P, the anisotropy decreased very rapidly and returned to the value of the free Ser15P peptide when the concentration reached 1:1 stoichiometry with p300. This suggests total displacement of the Ser15P peptide from the complex by an equal concentration of Thr18P. This indicates a much higher binding affinity of Thr18P as compared with Ser15P with p300. On the other hand, p53-(1–39) only weakly displaced Ser15P from the p300 complex. Even a 10-fold molar excess was not able to displace it fully (displacement may be only 50%, as can be estimated from anisotropy value), indicating at least several-fold weaker affinity. Two papers have attempted to estimate binding affinities of phosphorylated p53 protein (21, 23). It appears that Ser-15 phosphorylated p53 binds much more tightly than the unphosphorylated one and Thr18P also binds very tightly compared with Ser15P. Thus, the isolated 1–39 domain faithfully reproduces the functional nature of the protein, indicating retention of functional integrity.

To find out if there were significant structural differences between p53-(1–39) fragment and the 1–73 domain, chemical shifts of both these fragments were compared (8). Almost complete assignment of unmodified p53-(1–39) fragment was made using standard two-dimensional homonuclear NOESY/TOCSY strategy (26). The chemical shift differences of the amide protons are shown in Fig. 2*A*. The differences are largely confined to the N- and C-terminal ends. The difference at the C-terminal end is readily reconcilable, as the 1–39 fragment contains a free α-carboxyl group whereas the 1–73 fragment consists of continuing peptide chain. The difference in the N terminus is likely to arise from the additional residues and N-terminal modification of the recombinant protein (8). Only two residues, 16 and 28, in the middle showed greater than 0.1 ppm difference in chemical shifts. The implications of this observation are not clear, although indirect effects of extra residues in the N terminus cannot be completely ruled out. Thus, clearly the 1–39 fragment is similar to the 1–73 domain in structure and it is unlikely that the 1–39 subdomain has any strong interaction with the rest of the domain.

Chemical shifts can also be used to compare structural differences between the phosphorylated and unphosphorylated domains. We have compared the chemical shifts of amide resonances of the unphosphorylated and three phosphorylated domains. Fig. 2 (*B–D*) shows the chemical shift differences for amide protons between p53-(1–39) and Ser15P, Thr18P, and Ser20P, respectively. In all three cases, the largest difference was seen for the phosphorylated Ser/Thr residue, as expected. In case of Thr18P, very significant shift was also observed for the proximal residues, Phe19 and Ser-20. Interestingly, relatively large shifts were seen for some residues, which are distant from the phosphorylation site. This distant effect was found in all three phosphorylated domains, but appeared to be more pronounced in Thr18P and Ser20P. Glu-28, Ser-37, Gln-38, and Ala-39 showed changes of chemical shift greater than 0.1 ppm. In the case of Ser20P, modest chemical shift changes were seen throughout residues 21–30. All the residues were fairly distant from the modification site, suggesting long range interactions present in the domain. In particular, the residues at the C-terminal end, Ser-37, Gln-38, and Ala-39, are so distant from the phosphorylation site that secondary structure-mediated change can be ruled out.

Another parameter that may reflect conformational change is the coupling constant between NH and CαH ($J_{\text{NH-}\alpha\text{H}}$). This coupling constant tends to have a low value (~4–5 Hz) when the Ramachandran angle (ϕ) is in the helical range and a high value (~8–9 Hz) when the Ramachandran angle is in the extended conformation range. Thus, for relatively mobile peptide chains, perhaps lacking a unique conformation, a change in the value of $J_{\text{NH-}\alpha\text{H}}$ may be a reflection of a change in the distribution among different conformations. Fig. 3 shows the difference of $J_{\text{NH-}\alpha\text{H}}$ values between p53-(1–39) and Ser15P and Ser20P. It is clear that relatively large changes (~2 Hz) in the value of $J_{\text{NH-}\alpha\text{H}}$ occurred. The changes appear to be confined to the central part of the molecule (between residues 16–28) and

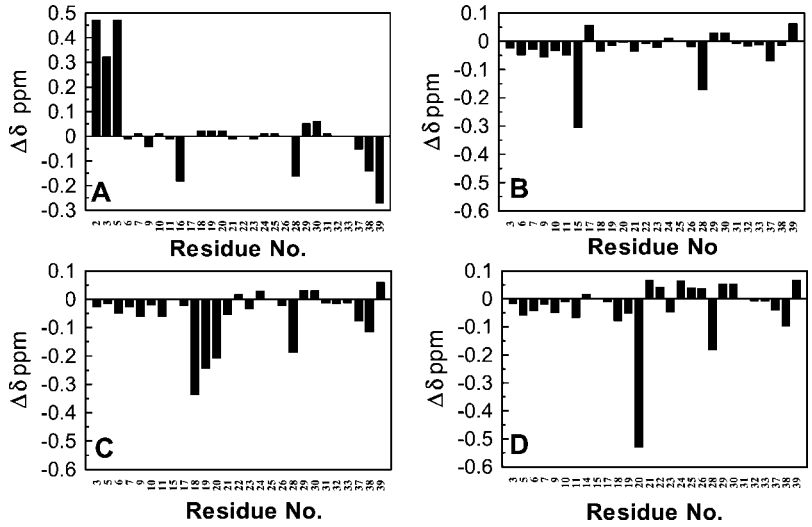

FIG. 2. **Comparison of chemical shifts of amide protons of different p53 N-terminal domains.** *A*, chemical shift difference of p53-(1–39) domain and recombinant p53-(1–73) domain at 5 °C. Chemical shifts of p53-(1–73) domain were taken directly from Lee *et al.* (6). p53-(1–39) chemical shifts were obtained from TOCSY spectra using water as standard. Chemical shift differences between the unphosphorylated p53-(1–39) domain and three phosphorylated derivatives: Ser15P (*B*), Thr18P (*C*), and Ser20P (*D*). The chemical shifts were obtained from standard NOESY/TOCSY assignment procedure at 27 °C. All the spectra were taken in 10 mM phosphate buffer, pH 7.0, containing 100 mM NaCl. Seven prolines are not shown for obvious reasons. Several resonances have zero chemical shift differences and hence do not appear as a *bar* in the figure.

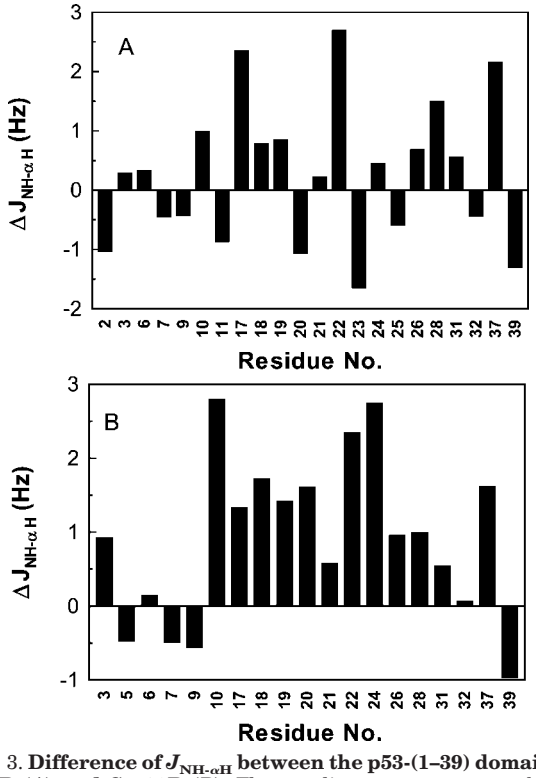

FIG. 3. **Difference of $J_{NH-\alpha H}$ between the p53-(1–39) domain and Ser15P (*A*) and Ser20P (*B*).** The coupling constants were obtained from double quantum-filtered COSY using the algorithm of Kim and Prestegard (21). The temperature was 27 °C. The spectra were taken in 10 mM phosphate buffer, pH 7.0, containing 100 mM NaCl. Prolines and residues that cannot be assigned unambiguously have not been shown.

the C-terminal residues. This pattern is very similar to the changes in the chemical shift, supporting long distance structural changes upon phosphorylation.

From a number of studies, it is now well established that tryptophan fluorescence in proteins is a sensitive probe of folding and tertiary structure (27). A number of fluorescence properties are sensitive to environment and solvent accessibility, two of which are fluorescence emission maximum and Stern-Volmer constant for collisional quenching. To assess the folded nature of the domain, we have measured fluorescence properties of the only tryptophan present at position 23. This is in the central part of the helix that spans the residues 17–26 (6) and is close to many of the phosphorylation sites in this domain. It is an important determinant for the Mdm2 interaction and possibly the p300/CBP interaction (4, 28). Thus, environment of this tryptophan residue may shed light on many important aspects of structure and function of this domain. The emission maxima of the unphosphorylated p53-(1–39) and Ser15P, Thr18P, and Ser20P are 341, 343, 350, and 350 nm, respectively (Table I). Fig. 4 shows the acrylamide quenching pattern (Stern-Volmer plots) for all the above mentioned domains. It is clear that the plots are linear in most cases and can be fitted well to a Stern-Volmer equation with a single class of fluorophore. K_{sv} (Stern-Volmer constant) of the domains are 3.9, 8.0, 11.0, and 11.2 M^{-1} for unphosphorylated, Ser15P, Thr18P, and Ser20P, respectively. As a control we have determined the K_{sv} values of a peptide consisting of residues 17–28 (Pep53) and the same peptide with five Aib substitutions (Bpep53). Aib substitutions were made to predispose the peptide into a more helical conformation. CD and NMR spectra indicate that Bpep53 is in a helical conformation (data not shown). In both the above mentioned peptides, the Stern-Volmer constants are high, 15.3 and 19.7 M^{-1} for Pep53 and Bpep53, respectively. The emission maxima are ~350 nm in both cases. Clearly, the K_{sv} of the tryptophan undergoes a dramatic reduction in going from Pep53, a largely random coil, to p53-(1–39). Even induction of helix by insertion of Aib does not reduce the K_{sv} or shift the emission maximum. Thus, the blue-shifted emission maximum in the p53-(1–39) fragment and lowering of K_{sv} may be the result of long range interactions. The long range interactions result in a folded conformation, which shields Trp-23 from solvent. Change in the K_{sv} value upon phosphorylation suggests a change in environment, and the corresponding red shift of emission maximum suggests that this change leads to an increased exposure of Trp-23. Properties of all the domains are summarized in Table I. Interestingly, for p53-(1–39), the Stern-Volmer plot is somewhat nonlinear, perhaps indicating the presence of multiple conformations. The *inset* shows the emission maximum shift as a function of increasing acrylamide concentrations for p53-(1–39). The shift of emission maximum for a single tryptophan protein (without tyrosine as well)

TABLE I
Properties of transactivation domain of p53 and its different phosphorylated derivatives

Domain	K_{SV}	Emission maximum	Perrin factor	Axial ratio
	M^{-1}	*nm*		
p53-(1–39)	3.9	341	1.33	7.5
Ser15P	8.0	343	1.42	10.0
Thr18P	11.0	350	1.40	9.5
Ser20P	11.2	350	1.43	10.0

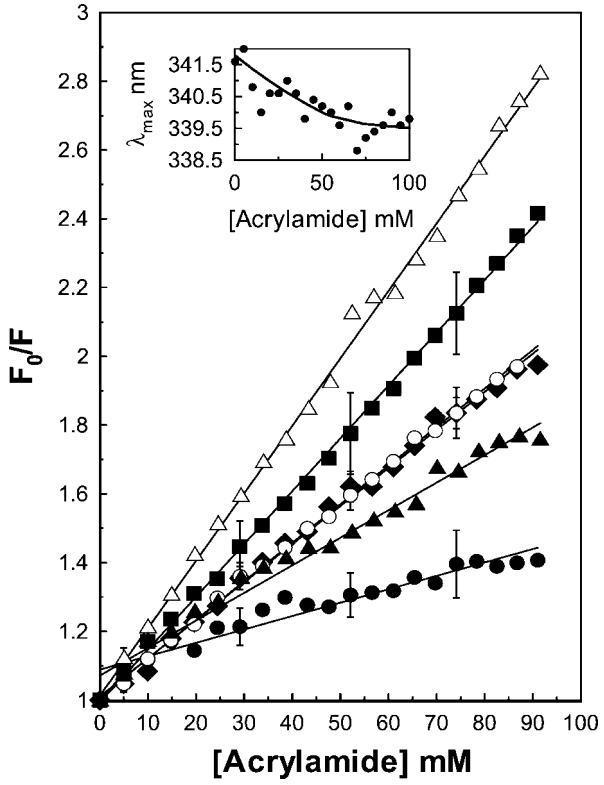

FIG. 4. **Stern-Volmer plots of acrylamide quenching of the tryptophan fluorescence of p53-(1–39) (●), Ser15P (▲), Thr18P (♦), Ser20P (○), Pep53 (■), and Bpep53 (△).** The excitation wavelength was 295 nm, and the emission was noted at 340 nm. The spectra were recorded at ambient temperature, which was 25 ± 1 °C. The solution conditions were 10 mM phosphate buffer, pH 7.0, containing 100 mM NaCl. The *inset* shows the emission maximum shift upon acrylamide quenching for p53-(1–39).

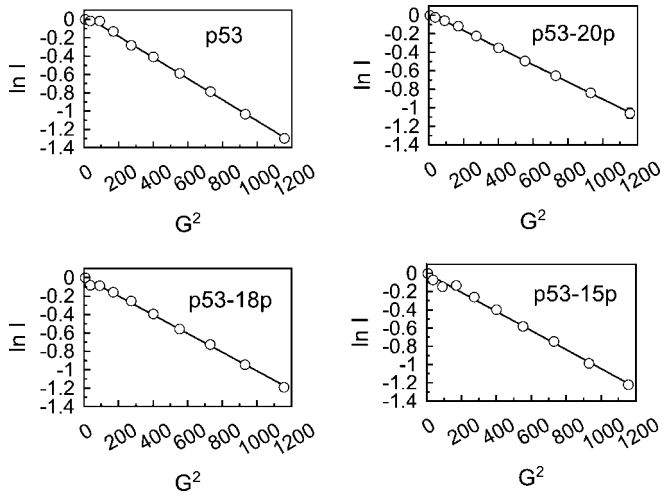

FIG. 5. **G^2 *versus* ln[intensity] plots for measurement of translational diffusion constant using pulse field gradient NMR for p53-(1–39) domain, Ser15P, Thr18P, and Ser20P, as labeled.** The experiment was performed using a stimulated echo-based pulse sequence. The measurements were carried out at 27 °C in 10 mM phosphate buffer, pH 7.0, containing 100 mM NaCl. The unit for field strength was gauss/cm. Based on three independent measurements, we estimate that standard errors are ~1%.

TABLE II
Diffusion constants of p53-(1–39) domain and its phosphorylated derivatives

Domain	Concentration	Diffusion constant ($\times 10^6$) $D_{20,w}$
	μM	$cm^2\ s^{-1}$
p53-(1–39)	280	1.31 ± 0.02
p53-(1–39) 15P	109	1.21 ± 0.01
p53-(1–39) 20P	854	1.19 ± 0.02
p53-(1–39) 20P	427	1.21 ± 0.01
p53-(1–39) 20P[a]	214	1.24
p53-(−39) 18P	990	1.27 ± 0.02
p53-(−39) 18P	495	1.22 ± 0.00[b]

[a] Because of the extremely diluted nature, only two determinations could be performed. In all other cases, three or four independent experiments were done.

[b] The standard error calculates to 0.004, but was approximated to zero in the second decimal place.

strongly supports presence of multiple conformations for the p53-(1–39). For the other phosphorylated fragments, no significant emission maximum shift could be detected (data not shown).

Pulse field gradients NMR can be used to measure translational diffusion constants, which are directly related to the hydrodynamic properties (29). Translational diffusion constants thus can be used to measure hydrodynamic properties of the transactivation domain and its phosphorylated derivatives, which in turn may shed some light on the compactness of the domains and states of aggregation. Fig. 5 shows the G^2 *versus* ln[intensity] plots for the unphosphorylated and the three phosphorylated domains. All the diffusion constants are summarized in Table II. The translational diffusion constant at 20 °C ($D_{20,w}$) of the unphosphorylated p53-(1–39) is 1.31×10^{-6} $cm^2\ s^{-1}$. This value is between that of sucrose and ribonuclease A and consistent with a monomer of molecular mass of 4.35 kDa (30). The compactness of the domain can be gauged from the fact that an unstructured 13-residue peptide has nearly the same diffusion constant and hydrodynamic radius (31) (1.54×10^{-6} $cm^2\ s^{-1}$; see below for the axial ratios). Thus, the stabilization of the tertiary structure in the 1–39 domain is likely to be from intramolecular interactions rather than intermolecular ones. The Ser-15 phosphorylated domain has a diffusion constant of 1.21×10^{-6} $cm^2\ s^{-1}$, ~8% lower than the unphosphorylated one. The Thr18P diffusion constant is also similar ($1.22–1.27 \times 10^{-6}$ $cm^2\ s^{-1}$) as is the diffusion constant for Ser20P ($1.19–1.24 \times 10^{-6}$ $cm^2\ s^{-1}$), all significantly different from the unphosphorylated case. Determination of diffusion constants at different concentrations does not show any significant change or trends, indicating that no significant aggregation occurs. This indicates that, upon phosphorylation, the compactness of the 1–39 domain is partially lost. If one assumes average hydration (0.34 g of water/g of protein) and partial specific volume (0.73 cm^3/g), one can qualitatively evaluate the shape of the protein through the Perrin factor, F (30). Table I lists the Perrin factors and the axial ratios of the corresponding ellipsoids. For the unphosphorylated 1–39 domain, the ratio is ~1:7.5 (for prolate as well as oblate ellipsoids) indicating a nonspherical shape. In contrast, a completely unstructured 13-residue peptide gave an axial ratio value of ~1:20 by the same technique (31). A much longer peptide chain, such as p53 transactivation domain, if completely disordered, should give even higher axial ratios. Thus, we may

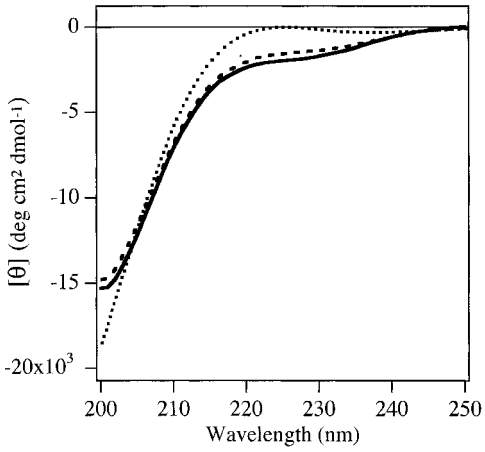

FIG. 6. **Circular dichroism spectra of unphosphorylated p53-(1–39) domain (——), Ser15P (– – –), and Pep53 (- - -).** All spectra were taken at 7.5 °C in 10 mM phosphate buffer, pH 7.0, containing 100 mM NaCl. The spectra were collected with a 2-mm path length cuvette, around which chilled water was circulated. The temperature of the sample was recorded by placing a thermocouple in the cuvette. Bandwidth was 2 nm, and the scan speed was set at 20 nm/min. The spectra shown here are smoothed.

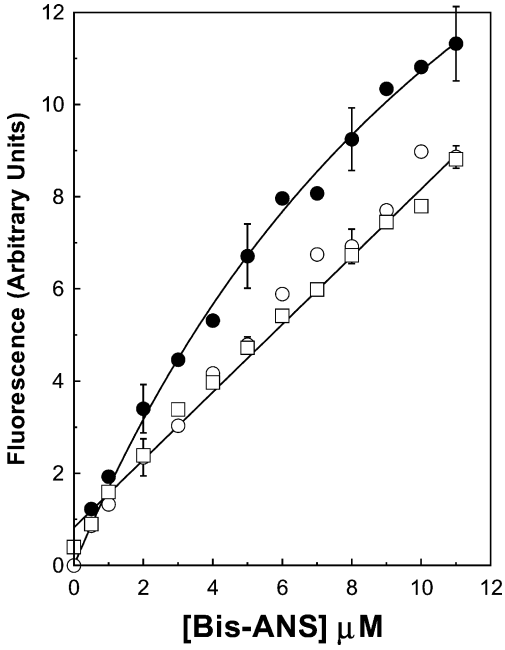

FIG. 7. **Bis-ANS titration of 10 μM p53-(1–39) (●), Ser20P (○), and buffer (□).** The solution conditions were 10 mM phosphate buffer, pH 7, containing 100 mM NaCl. The temperature was 25 ± 1 °C. Excitation wavelength was 387 nm, and the emission wavelength was 490 nm. The lines are fit with linear and hyperbolic equations and do not signify any binding model. The *error bars* were derived from three independent experiments. For clarity, only every *third error bar* is shown.

conclude that p53-(1–39) has a folded conformation to some degree. Phosphorylations increase the axial ratio. This indicates a more open conformation of the phosphorylated domains.

To assess the secondary structural content of the domain in the phosphorylated and unphosphorylated states, we have measured the far-UV CD spectra. Small peptides display considerable flexibility and predisposition only to certain conformations. To accentuate the conformational preferences, peptide CD spectra are often taken at lower temperatures. Hence, we have measured CD spectra at 7.5 °C. Fig. 6 shows the CD spectra of the unphosphorylated and Ser-15 phosphorylated p53-(1–39). The CD spectrum of the unphosphorylated domain exhibits small but significant mean residue ellipticity at 222 nm and a pronounced minimum around 200 nm. Considering that the solution conformation of the domain to be an equilibrium mixture of α-helix (characterized by a double minima at 208 and 222 nm) and an extended conformation (characterized by a pronounced minimum at 190 nm), the CD spectrum of the unphosphorylated domain suggests the presence of some fraction of helical population. Upon phosphorylation, the absolute CD intensity decreases slightly but with no change in spectral shape, indicating very little change in secondary structure. The other two phosphorylated domains show Ser15P like CD spectra under similar conditions (data not shown). Interestingly, the peptide Pep53 has no significant negative band at 222 nm and its CD spectrum resembles that of an extended conformation. Previous NMR studies have suggested that the domain 1–73 contains a helix spanning residues 17–26 (6). This is consistent with significant helical content of the fragment p53-(1–39). The lack of any significant helical content of the peptide Pep53 may therefore suggest the presence of long range interactions in the 1–39 domain that stabilizes the helix.

Bis-ANS is widely used as a probe for hydrophobic regions of proteins. The general experience with bis-ANS and ANS is that they are incapable of binding to completely unfolded states. This is evident from no detectable binding to proteins at conditions that completely unfold the proteins (32). The hydrophobic patches in proteins that are thought to be important for binding of this class of fluorescent probes require some organized structure to bring hydrophobic elements in a protein chain in close proximity. We have thus probed organized structure using bis-ANS binding as a probe in p53-(1–39) and its Ser-20 phosphorylated counterpart. Fig. 7 shows the binding isotherms. It is clear that Ser20P is almost identical to the buffer control suggesting no binding. On the other hand, there is a significant additional fluorescence enhancement with p53-(1–39). This provides additional support that the unphosphorylated domain has some elements of a folded structure, which disappears or reduces upon phosphorylation.

The presence of long range interactions in the transactivation domain of p53 raises an interesting question about its nature. The NMR study indicated that the central helix extends up to residue Leu-26 (6). The stretch of four contiguous residues (PENN) that follow the helix has a high probability of turn formation. A search for such a sequence (LPENNV) through Protein Data Bank revealed five proteins that have such a sequence with only one sequence mutation. In all such cases, the residues adopt a turn conformation (Protein Data Bank identification codes 1cpb, 1f4b, 1js4, 1sky, and 1ehi). If the residues LPENNV adopt a turn in the p53 transactivation domain, several C-terminal residues may interact with residues at the N-terminal side of the domain. This is consistent with the observation that the last three residues show significant chemical shift change upon phosphorylation that appears to result in a more open structure. Why the phosphorylations lead to more open states is not known at present. However, in Thr18P, the hydroxyl group of Thr-18 may hydrogen-bond to NH or to the β-COOH group of Asp-21, contributing to the stability of the helix. Phosphorylation would eliminate such hydrogen bonds and in addition would cause charge repulsion, destabilizing the helix.

One of the general mechanisms of transcription activation in eukaryotes is by acetylation of histones and consequent increased accessibility of the DNA toward proteins that includes the transcription initiation machinery (33, 34). One of the functions of the transcription activation factors such as p53 is to localize itself in an appropriate region through sequence-specific DNA binding activity and recruit a histone acetyltransferase such as p300/CBP in the locality (35). How this recruit-

ment occurs is not well understood in terms of structural or energetics principles. Activation of p53 in response to genotoxic stress results in transcription activation from a number of promoters. The N-terminal domain of p53 is the domain responsible for interaction with p300/CBP and its recruitment (36). It has been suggested that the strength of interaction between the transactivation domain and its partners correlates with the degree of transcription activation (37). In case of Ser15P, it has been shown that phosphorylation leads to enhanced interaction with CBP (28). The structural basis of this enhanced interaction remains unclear.

Many transactivation domains are known to be acidic and flexible (38). Flexibility implies a rapidly interconverting distribution of states. However, little is known about their structures. The p53 transactivation domain falls into this general category. Recently, NMR studies have indicated that this domain has defined secondary structures. Based on lack of long range nuclear Overhauser effects, it was suggested that the domain lacks organized tertiary structure (8). Fluorescence results and hydrodynamic properties reported here, however, argue for presence of long range interactions and a folded structure. Change of chemical shifts of residues distant from the phosphorylation sites also argues in favor of long range interactions. We believe that lack of long range nuclear Overhauser effects results from the flexible nature of the domain and a consequent reduction of correlation time rather than an unfolded conformation. Flexibility is also known in other domains. It has been argued that such flexible structures allow those domains to fit into "molds" of different receptor structures (39). This increase in ability to recognize different targets comes at a cost of binding affinity as the entropic barrier for a disorder-order transition has to be overcome. A similar argument can be advanced here. We propose that the flexible transactivation domain of p53 is composed of rapidly equilibrating conformers, one quasi-globular and the others relatively open. We have observed that fluorescence quenching of p53-(1–39) leads to significant blue shift of the emission maximum, suggesting multiple environments for the single tryptophan residue. It has been proposed that transactivation domains interact with multiple partners through semispecific hydrophobic regions (37). In case of p53, the central helix appears to be the critical interaction point (40). In a folded structure, where the helix may be partially shielded, the interaction energy with the partner proteins may be reduced. Phosphorylations at different positions shift the equilibrium toward the open forms to various degrees, causing enhancement of protein-protein interaction.

CONCLUSION

By several techniques we have shown that the transactivation domain of p53 has a folded structure. It is likely that this folded structure is mobile and lacks organized tertiary interactions. Folded structures without organized tertiary interactions are well known in proteins, of which molten globules are the most ubiquitous. Such dynamic folded structures may be important for proteins that interact with multiple receptors.

Acknowledgments—We acknowledge the help of Dr. Soumen Basak and Jaganmoy Guin for the measurement of CD spectra and the help of Barun Mazumdar for the measurement of NMR spectra. We also thank Asim Banerjee for help with HPLC. Dr. Kundu thanks L. Kraus and J. T. Kadonaga for the baculovirus expression vector.

REFERENCES

1. Appella, E., and Anderson, C. W. (2000) *Pathol. Biol.* (*Paris*) **48,** 227–245
2. Puri, P. L., Maclachlan, T. K., Levero, M., and Giordano, A. (1999) in *The Molecular Basis of Cell Cycle and Growth Control* (Stein, G. S., Baserga, R., Giordano, A., and Denhardt, D. T., eds) pp. 15–79, Wiley-Liss, New York
3. Ljungman, M. (2000) *Neoplasia* **2,** 208–225
4. Kussie, P. H., Gorina, S., Marechal, V., Elenbaas, B., Moreau, J., Levine, A. J., and Pavletich, N. P. (1996) *Science* **274,** 948–953
5. Sterner, D. E., and Berger, S. L. (2000) *Microbiol. Mol. Biol. Rev.* **64,** 435–459
6. Jeffrey, P. D., Gorina, S., and Pavletich, N. P. (1995) *Science* **267,** 1498–1502
7. Rustandi, R. R., Baldisseri, D. M., and Weber, D. J. (2000) *Nat. Struct. Biol.* **7,** 570–574
8. Lee, H., Mok, K. H., Muhandiram, R., Park, K. H., Suk, J. E., Kim, D. H., Chang, J., Sung, Y. C., Choi, K. Y., and Han, K. H. (2000) *J. Biol. Chem.* **275,** 29426–29432
9. Stewart, Z. A., Tang, L. J., and Pietenpol, J. A. (2001) *Oncogene* **20,** 113–124
10. Damia, G., Filiberti, L., Vikhanskaya, F., Carrassa, L., Taya, Y., D'incalci, M., and Broggini, M. (2001) *Neoplasia* **3,** 10–16
11. Bean, L. J., and Stark, G. R. (2001) *Oncogene* **20,** 1076–1084
12. She, Q. B., Chen, N., and Dong, Z. (2000) *J. Biol. Chem.* **275,** 20444–20449
13. Dumaz, N., Milne, D. M., and Meek, D. W. (1999) *FEBS Lett.* **463,** 312–316
14. Sakaguchi, K., Saito, S., Higashimoto, Y., Roy, S., Anderson, C. W., and Appella, E. (2000) *J. Biol. Chem.* **275,** 9278–9283
15. Unger, T., Sionov, R. V., Moallem, E., Yee, C. L., Howley, P. M., Oren, M., and Haupt, Y. (1999) *Oncogene* **18,** 3205–3212
16. Jabbur, J. R., Huang, P., and Zhang, W. (2000) *Oncogene* **19,** 6203–6208
17. Chehab, N. H., Malikzay, A., Stavridi, E. S., and Halazonetis, T. D. (1999) *Proc. Natl. Acad. Sci. U. S. A.* **96,** 13777–13782
18. Kraus, W. L., and Kadonaga, J. T. (1998) *Genes Dev.* **12,** 331–342
19. Canet, D. (1996) *Nuclear Magnetic Resonance: Concepts and Methods*, John Wiley & Sons, New York
20. Cantor, C. R., and Schimmel, P. R. (1980) *Biophysical Chemistry*, Vol. II, p. 584, W. H. Freeman & Co., San Francisco
21. Kim, Y., and Prestegard, J. H. (1990) *Proteins* **8,** 377–385
22. Garel, J. R. (1976) *Eur. J. Biochem.* **70,** 179–189
23. Sakaguchi, K., Herrera, J. E., Saito, S., Miki, T., Bustin, M., Vassilev, A., Anderson, C. W., and Appella, E. (1998) *Genes Dev.* **12,** 2831–2841
24. Uesugi, M., and Verdine, G. L. (1999) *Proc. Natl. Acad. Sci. U. S. A.* **96,** 14801–14806
25. Dornan, D., and Hupp, T. R. (2001) *EMBO Rep.* **2,** 139–144
26. Wuthrich, K. (1986) *NMR of Proteins and Nucleic Acids*, John Wiley & Sons, New York
27. Lakowicz, J. R. (1999) *Principles of Fluorescence Spectroscopy*, 2nd Ed., Kluwer Academic/Plenum Publishers, New York
28. Gu, W., Shi, X. L., and Roeder, R. G. (1997) *Nature* **387,** 819–823
29. Wilkins, D. K., Grimshaw, S. B., Receveur, V., Dobson, C. M., Jones, J. A., and Smith, L. J. (1999) *Biochemistry* **38,** 16424–16431
30. Cantor, C. R., and Schimmel, P. R. (1980) *Biophysical Chemistry*, Vol. II, 1st Ed., W. H. Freeman & Co., San Francisco
31. Pal, D., Mahapatra, P., Manna, T., Chakrabarti, P., Bhattacharyya, B., Banerjee, A., Basu, G., and Roy, S. (2001) *Biochemistry* **40,** 15512–15519
32. Das, B. K., Bhattacharyya, T., and Roy, S. (1995) *Biochemistry* **34,** 5242–5247
33. Nakayama, T., and Takami, Y. (2001) *J. Biochem.* (*Tokyo*) **129,** 491–499
34. Davie, J. R., and Moniwa, M. (2000) *Crit. Rev. Eukaryot. Gene Exp.* **10,** 303–325
35. Ptashne, M., and Gann, A. (1997) *Nature* **386,** 569–577
36. Grossman, S. R. (2001) *Eur. J. Biochem.* **268,** 2773–2778
37. Melcher, K. (2000) *J. Mol. Biol.* **301,** 1097–1112
38. Nagadoi, A., Nakazawa, K., Uda, H., Okuno, K., Maekawa, T., Ishii, S., and Nishimura, Y. (1999) *J. Mol. Biol.* **287,** 593–607
39. Kriwacki, R. W., Hengst, L., Tennant, L., Reed, S. I., and Wright, P. E. (1996) *Proc. Natl. Acad. Sci. U. S. A.* **93,** 11504–11509
40. Gu, W., and Roeder, R. G. (1997) *Cell* **90,** 595–606